This is a repository copy of *Load Control of a 300 hp Tunneling Machine*.

White Rose Research Online URL for this paper:
http://eprints.whiterose.ac.uk/76374/

Monograph:
Edwards, J.B. (1983) Load Control of a 300 hp Tunneling Machine. Research Report.
ACSE Report 220 . Department of Control Engineering, University of Sheffield, Mappin
Street, Sheffield

LOAD-CONTROL OF A 300 h.p. TUNNELLING MACHINE

by

J.B. Edwards

Department of Control Engineering,
University of Sheffield,
Mappin Street, Sheffield S1 3JD.

Research Report No. 220

April 1983

LOAD-CONTROL OF A 300 h.p. TUNNELLING MACHINE

by

J.B. Edwards

Department of Control Engineering,
University of Sheffield,
Mappin Street, Sheffield S1 3JD.

Research Report No. 220

April 1983

SUMMARY

In response to a request from the National Coal Board, a mathematical
model is derived for the rock-cutting operation of a 300 h.p. tunnelling
machine currently in use at Cadley Hill Colliery. The existing over-
riding load control system is shown to produce oscillatory load patterns
when cutting harder rock that accord closely with preliminary observa-
tions underground.

The model is used to design and confirm the performance of an
improved load control system using derivative power feedback. The
necessary modifications to the existing control amplifier should be
fairly straightforward.

1. INTRODUCTION

1.1 Machine Description and Operation

The rock tunnelling machine under investigation and presently operating at Cadley Hill Colliery is illustrated diagrammatically in Fig. 1. The machine is of the boom type (rather than the alternative full-face-cutter type) and excavates a tunnel of circular cross-section by the following sequence of operations:-

(a) With the boom in a central position, the rotating cutting head is sumped into the rock to its full depth (0.75m) by hydraulic pushing rams.

(b) Under the action of the boom-tilting jacks shown, the boom is moved outwards to a radius R equal to about 40% that of the finished tunnel.

(c) The whole boom assembly is now rotated at a peripheral speed, v, to complete an annular cut of mean radius, R.

(d) Radius R is now increased to a value close to that of the finished tunnel (5.5m) and a second annular cut made in the reverse direction so as to avoid progressive twisting of the power cable feeding the cutting-head motor.

(e) The sequence (a) to (e) is repeated following a second sumping operation before it becomes necessary to advance the machine as a whole. (The machine is not shown in its entirety in Fig. 1 but, behind the boom assembly, the machine carries an elaborate system for installing segmental concrete ring supports for the tunnel which are installed in parallel with the cutting operations).

1.2 Gearbox Failures

Over several months operation, a number of failures of the epicyclic reduction gear-box (1500: 6r.p.m.) via which the cutting head

is driven from a 300 h.p. squirrel cage induction motor (Fig. 1) have occurred requiring several enormously expensive replacements. This report is the first of a series outlining an investigation being carried out at Sheffield into the likely causes of these failures and possible means for their avoidance in future.

1.3 Existing Load Control

The existing load control system is of an overriding, or limiting type: a preset reference value v_r for rotational speed v is compared with a potentiometer measurement of the angle of the swash plate of the variable delivery pump feeding the boom-rotating drive motor and the error signal used to deflect the spool of an electrohydraulic servo-valve which directs oil, at system pressure, to the appropriate swash tilting cylinder. A speed v, very nearly equal to v_r, is thus attained very rapidly provided the load P_i on the cutting motor, produced by v_r and as measured by a power transducer, does not exceed a load reference setting P_r (ideally $\equiv$ the 300 h.p. rating of the motor). Should $P_i - P_r$ become positive (i.e. load exceed reference) as detected by a diode in the feedback of the comparator amplifier, then a preset proportion of this error is applied to back off the servo valve signal thus reducing pump delivery and hence speed v.

Detailed recordings are awaited, but the system is observed to oscillate in practice when v_r, the so-called rate reference, is set high and the machine is cutting rock rather than coal. The load oscillations observed on the motor monitoring the transducer are not excessive (say $\pm$ 20% P_r) but the swash angle and speed v are observed to fluctuate between zero and values well in excess of the average. The observed frequency of oscillation is one cycle in about 3.0 seconds.

Complete stabilisation of the load control system is therefore an obvious objective that should be sought as a means of controlling

more precisely the average power consumption of the motor and hence the average load transmitted by the gear-box.

1.4 Additional Causes of Load Fluctuation

Although not apparent on the load meter, further components of load oscillation at much higher frequencies of the order of 10 Hertz are perceptible through the obvious vibration that occurs when cutting hard material. These are the result of chatter resulting from interaction of the cutting dynamics and the stiffness dynamics of the boom-structure, boom-drive and cutting-head-drive. A fuller study of these vibrations is necessary to ascertain their amplitude, and therefore their serious-ness both on the machine as it now exists and on a modified control system whose behaviour could be degraded by the chatter. This will be the topic of subsequent analysis in a future report. The present report confines attention to improved control of the chatter-free machine.

A further cause of load variation is the heap of cut material that accumulates at the bottom of the cut face prior to its discharge via the scraper chain conveyor running beneath the boom and machine body (not shown in Fig. 1). As the boom ploughs through this heap at the bottom of the cut, particularly on its second sweep, a large additional drag is imposed by the recirculated material. No attempt is made in this first report to model this phenomenon and the following analysis is therefore confined to cutting operations made above this heap, i.e. through the top 270° of boom travel.

2. MODELLING THE SYSTEM

The following model is developed from ideas first published by the author in References (1) (2) and (3) (section 6). The numerical values used in the preliminary model are 'first estimates' and will require some adjustment in future as more complete data becomes available.

2.1 The Cutting Dynamics

These dynamics relate the boom speed, v to the power P_m supplied by the gear-box under investigation to the cutting head shaft. The 'bite' y made by each spiral line of cutting picks (Fig. 1) will be described by

$$dy/dt = v(t) - v(t-T) \tag{1}$$

where T is the time delay between the arrival of successive picks (in the same plane). Given a cutting head speed of 6 r.p.m. and that there are 6 spiral starts per revolution, T works out to be $60/(6 \times 6) = 1.67s$ but a rounded value of 1.8s is used here, partly for convenience of simulation and partly to allow for some nominal slip in the induction motor since the 6 r.p.m. corresponds to 1500 r.p.m. synchronous speed.

For simplicity it is here assumed that the cutting load P_m is proportional to bite y,

$$\text{i.e. } P_m = k_h y \tag{2}$$

the constant of proportionality k_h depending on R and on pick sharpness and the hardness of the rock being cut. A nominal value for k_h has been determined as follows:

A brief inspection of the machine cutting operations indicated the uninterrupted boom revolution time to be about 18 min. when operating at a load P_m of 160 kw ($\equiv$ to $P_e = 200$ kw if the motor and gear-box efficiency is taken to be 80% overall). Taking the mean circumference $2\pi R$ of the annular cut to be 30 m thus yields a nominal value for $\bar{v} = 30/(18 \times 60) = 1/36$ m/s and hence an average bite $\bar{y} = \bar{v} T = 1.8/36 = 0.05$m (i.e. 5.0 cm). Thus an acceptable nominal value for k_h would appear to be $160/0.05 = 3200$ kw/m.

2.2 Induction Motor Inertia Lag

The dynamic relationship between input power P_i to the induction motor and output power P_m may be approximately modelled by a first-order lag thus

$$P_e = k_1 P_m / (1 + T_m D) \tag{3}$$

where k_1^{-1} is the overall motor and gear-box efficiency so that k_1 is here set at $0.8^{-1} = 1.25$ and T_m is the time constant of the motor's rotor, cutting head and gear-box: the former being dominant because of the enormous reduction ratio. $D = d/dt$ and T_m is given by

$$T_m = - J / (\partial \tau / \partial \Omega) \tag{4}$$

where $\partial \tau / \partial \Omega$ is the slope of the motor's torque-speed characteristic, being measured in radians p.u. time.

Now assuming that, as is normal, peak torque, τ_m, = 2.5 full load torque, here = 2.5 . 200 = 500 synchronous kw and that peak torque occurs at about 10% slip, i.e. when slip, $\Delta \Omega \equiv$ 150 r.p.m. then

$$\frac{\partial \tau}{\partial \Omega} \simeq - \frac{\tau_m}{\Delta \Omega} = - \left(\frac{500. \ 10^3 . \ 60}{2 \pi . \ 1500} \right) \left(\frac{60}{150. \ 2\pi} \right)$$

= 203 N.m./s

Now the motor's moment of inertia is given as 4.89 kg m^2 and allowing a further 100% for other rotating parts makes J = 9.78 kg m^2. Thus from equation (4) T_m works out to be 9.78/2.03 = 0.048s.

2.3 Electrohydraulic Servo System

The swash-plate pump and servo-valve can be regarded as being basically an integrator (since the rate of swash travel, and hence the rate-of-increase of v, will be proportional to valve-opening). The feedback from the swash potentiometer, inbuilt into the control system around this integrator, renders the system model again as a first-order lag. (The valve itself, having a bandwidth if 50 → 100 Hertz, can be regarded as being virtually instant-acting in this application). The system can therefore be modelled thus:

$$v = k_2 P_e / (1 + T_h D) \tag{5}$$

where P_e is the power error signal (here measured in kw) entering the servo amplifier (driving the servo valve) and k_2 is the overall gain (sensitivity) of the electronic and electrohydraulic amplifier system. The lag T_h has yet to be determined either from a recorded step response or from valve and servo cylinder capacitance data. Initial inspection at Cadley Hill suggested a rapid response in this part of the system and a value of $T_h = 0.25s$ has been assumed initially. The value of k_h is, of course, readily adjustable.

2.4 Overall System Model and Existing System Performance Prediction

Combining the individual component models of the hydraulics, the cutting head, its drive motor and the controller yields the block diagram representation of Fig. 2. Varous alternative controllers are shown including the existing overriding controller. Also shown in Fig. 2 is an electronic smoothing filter for the removal of a.c. ripple from the power transducer output. It is modelled by

$$P_i' = P_i / (1 + T_f D) \tag{6}$$

where P_i' is the filtered value of P_i and T_f is the filter time constant. To effectively remove the electrical ripple (50 Hertz) T_f need only have a value of about, $5/2\pi 50$, $\simeq 0.016s$, such a value being virtually negligible in the present context of overall system behaviour. The value of T_f actually used at present has yet to be determined and for the moment the above minimum value is assumed. The diagram provides the basis for a digital simulation of the system, the results of which are described fully in Section 4.

For the moment we consider only Fig. 3 which shows the predicted performance of the existing system with the rate reference v_r set to produce a speed v just less than that needed to bring in the overriding load control (P_r here being set at 200 kw). The desired steady speed

is clearly achieved following switch-on but halfway through the test
a 50% step increase in rock hardness (i.e. in k_h) is imposed so actuating
the load control. Clearly sustained oscillations of cycle-time $\simeq$ 4s occur.
This frequency is only very slightly slower than that observed, and, in
this connection, it should be noted that T_m was here set at an initially
estimated value of 0.5s not the updated figure of 0.048s calculated in
Section 2.2. Reducing T_m, which turns out not to have a dominant effect,
will obviously increase the predicted oscillation frequency so yielding
good correlation between simulation results and those observed on site.

It will also be noted from Fig. 3 that whereas P_i oscillates with
moderate amplitude ($\pm$ 38% P_r) in the harder material, v fluctuates much
more widely, i.e. between zero and k_h the value (= $P_r/k_h k_2 T$) at which
load control is activated. Both these amplitudes accord roughly with
initial observation. As proper recordings of P_i, swash angle and boom
rotation become available it should be possible to tune up the model of
Fig. 2 to produce predictions of improved accuracy. Present predictions
seem sufficiently accurate however, to permit the existing model to be
used as a basis for the initial design of controller improvements.

3. DESIGN OF LOAD CONTROL COMPENSATOR

3.1 Inverse Nyquist Locus

Assuming the use of a linear continuous controller of the form

$$v_r = k_1 (P_r - P_i') \tag{7}$$

then the overall open loop transfer function of the uncompensated system
is (from Fig. 1):

$$G(s) = \frac{P_i'}{P_r - P_i'} = \frac{k_1 k_2 k_h (1-e^{-Ts})}{(1+T_f s)(1+T_h s)(1+T_m s) \cdot s} \tag{8}$$

and, setting Laplace variable s = jω, where ω is the angular frequency
of any imposed error signal $P_r - P_i'$,   yields an inverse Nyquist

locus[*] of the form shown in Fig. 4. It is interesting to note from consideration of the locus (shown as a broken line) of the ideal case of $T_f = T_h = T_m = 0$ that the critical frequency ω_c at which unstable oscillations will occur (if gain $k_1 \, k_2 \, k_h$ is set sufficiently high) must lie in the range

$$\pi/T < \omega_c < 2\pi/T \qquad\qquad (9)$$

i.e. the critical oscillation period must lie in the range T to 2T (i.e. 1.8 to 3.6 seconds - similar to those observed on the actual machine).

3.2 Setting the Controller Gain

To achieve stability without significant slugging of the system it is necessary to reduce the system gain only until the critical 'minus-one point' on the locus of Fig. 4 is close to the point at which the real axis is crossed (i.e. at $\omega = \omega_c$). The locus is then to be deflected away from this critical condition by means of dynamic compensation networks designed in 3.3.

For the parameters assumed (T = 1.8s, T_m = 0.5s, T_h = 0.25s and T_f negligible) it is found that $\omega_c \simeq 2.09$ rad s^{-1} and at this frequency

$$\left| G(j\omega_c)^{-1} k_1 k_2 k_h \right| = \frac{\left| (1+T_m j\omega_c)(1+T_h j\omega_c) \right|}{\left| 1 - e^{-Tj\omega c} \right|} \, \omega_c \qquad\qquad (10)$$

$$= \frac{1.55 \quad 1.10 \quad 2.09}{1.89} \quad = 1.89$$

so that, to make $G(j\omega_c) = 1.0$, gain k_1 must be set to

$$k_1 = 1.89/k_2 k_h = 1.89/(1.25 \, . \, 3200) = 0.47.10^{-3} \text{ m/s/kw}$$

[*] i.e. a polar plot of $(P_r - P_i')/ P_i'$ in amplitude and phase as frequency ω is varied

In the simulations a value of $k_1 = 0.3.10^{-3}$ m/s/kw was used to allow a margin of safety.

3.3 Dynamic Compensator Design

To deflect the inverse Nyquist locus away from the critical minus one point to give a resonant closed-loop gain* $\simeq$ the static closed-loop gain, an added vector shift of approximately unit magnitude and 135° phase shift is needed at $\omega = \omega_c$ as Fig. 4 illustrates. To achieve this, it is proposed to employ an additional feedback from the power-transducer via a differentiating network of transfer-function

$$P_d/P_i' = k_d T_d s/(1+T_d s) \tag{11}$$

where P_d is a so called 'derivative power' feedback, and an additional forward path lag of transfer-function

$$P_e' = P_e/(1 + T_L s) \tag{12}$$

where

$$P_e = P_r - P_i' \tag{13}$$

the control law now taking the form:

$$v_r = k_1(P_e' - P_d) \tag{14}$$

rather than simply that of equation (7) i.e.

$$v_r = k_1 P_e \tag{15}$$

The added vector $V(s)$ will be given by

$$V(s) = \frac{k_d T_d s (1+T_L s)}{(1 + T_d s)} \tag{16}$$

so that $T_d \omega_c$ is chosen $<< 1.0$ to allow the differentiator to provide nearly 90° of phase advance whilst the additional lead ($\simeq 45^{\circ}$) is provided by the $(1 + T_L j \omega_c)$ term. We therefore set

$$T_d \omega_c = 0.2 \text{ , say}$$

$$\text{so that } T_d = 0.2/2.09 \qquad \boxed{\simeq 0.1s}$$

*The closed-loop gain i.e. between P_r and P_i' at any frequency ω is the reciprocal of the vector drawn from the critical -1 point to the locus at frequency ω.

Now for the correct slope of added vector, from equation (16)

$$- \tan^{-1} T_d \omega_c + 90^\circ + \tan^{-1} T_L \omega_c = 135^\circ$$

$$\therefore \tan^{-1} T_L \omega_c = 45^\circ + \tan^{-1} 0.209 = 56.8^\circ$$

$$\therefore T_l \omega_c = 1.53$$

so that $T_L = 1.53/2.09 = 0.73$ s. , $\boxed{\text{say 0.75s}}$

Hence length of added vector, @ $\omega = \omega_c$

$$= \frac{k_d \; 0.209 \quad |1 + j\, 1.53|}{1 + j\, 0.209} \quad = \frac{k_d}{2.69} = 1.0$$

$$\therefore \boxed{k_d = 2.69}$$

These parameter values were therefore employed in initial simulation studies the results of which are given in Section 4.

4. SIMULATION RESULTS

Simulation result for the existing overriding controller are shown in Fig. 3 and were discussed in Section 2.4. Some instability is clearly obvious.

. Fig. 5 shows the simulated performance of a proportional controller (i.e. equations 7 or 15) with the controller gain k_c set to $0.3 \cdot 10^{-3}$ i.e. a predicted stable value for a hardness coefficient of 3200 kw/m bite. Clearly the system is stable with this softer material but when the hardness is increased by 50% to 4800 kw/m bite (after 25 seconds) instability just occurs; in accordance with the predictions of Section 3.2. The reference P_r was set at 200 kw for Fig. 5 but clearly the average value of P_i obtained falls below this value. This is to be expected since analysis of the system readily reveals that, in steady state :

$$\frac{P_i}{P_r} = \frac{k_1 k_2 k_h T}{1 + k_1 k_2 k_h T} \tag{17}$$

so that, theoretically, the average values of P_i expected are 137 kw and 153 kw in the softer and harder rock respectively : both figures according with the simulation results of Fig. 5.

Fig. 6 shows the effect of stabilising the uncompensated proportional control system of equation 7 by reduction of controller sensitivity from $0.3 \ 10^{-3}$ to $0.15 \ 10^{-3}$ m/s/kw. Stability is now achieved under both hardness conditions as expected but with P_r again set at 200 kw. Thus, although stability can be achieved by gain reduction above, this is at the expense of control accuracy: a 50% change in rock hardness causing a 20% change in load.

The trade-off between stability and static accuracy is much improved by using the dynamic compensator of Section 3 as Fig. 7 shows. The controller gain k_1 was here returned to $0.3 \ 10^{-3}$ m/s/kw and the compensator parameters used were $k_d = 2.69$, $T_d = 0.1$ s and $T_L = 0.75$ s (i.e. identical values to those derived in Section 3). P_r was again set at 200kw. Stability is clearly now achieved <u>with</u> the higher system sensitivity so that now the 50% hardness increase causes only a 12% increase in P_i on average. (It is obvious of course that pick wear may be regarded as an equivalent increase in rock hardness and its effects will be similar in practice). The system response remains good and its static accuracy improved still further if k_1 is raised to $0.45 \ 10^{-3}$ m/s/kw.

Fig. 8 is identical to Fig. 6 (computed for the uncompensated proportional controller) but with P_r raised from 200 kw to 263 kw to make the steady-state value of $P_i = 137$ kw before the hardness increase i.e. as with the compensated system. As expected, the value of P_i now increases

to 163 kw after the 50% hardness change, compared to the 153 kw
of Fig. 7.

Finally Fig. 9 is included showing the performance of the uncompen-
sated system with the sensitivity raised to 0.5 10^{-3} m/s/kw yielding
unstable behaviour with the higher and lower hardness values. Load
oscillations are of unacceptable amplitude and rotational speed v
varies in a hopping manner similar to its behaviour with the existing
controller (Fig. 3). The results given would therefore appear to make
an excellent case for the compensated proportional controller (Fig. 7).

5.   CONCLUSIONS AND PROPOSALS FOR FURTHER WORK

A preliminary mathematical model has been derived for the rock-
cutting operation of the 300 h.p. tunnelling machine and initial estimates
for its parameter values have been derived. The performance of the model,
under the control of a model of the existing load controller, when
simulated on the digital computer, closely resembles that observed on
the actual machine underground producing low-frequency load oscillations
of about 4s cycle-time and ± 38% amplitude. Underground recordings of
power consumption and swash-plate pump angle are needed for fine tuning
of the model.

Frequency response analysis using the derived machine model shows
that responsive control without servo oscillation should be obtainable
by:

(a)   conversion to continuous control action

(b)   addition of derivative control action to the load feedback signal

and   (c)   insertion of a small lag in the power error path.

The findings are confirmed by simulation which also proves the modified
system to be widely tolerant of machine and controller parameter variation.

Further investigation must be conducted to examine the causes and
effects of the higher frequency chatter (16 Hertz or so) that is

discernable through machine vibration underground. It is unlikely that this can be compensated significantly by control action but its source would be worth knowling to aid future machine redesign. The chatter could upset the performance of the proposed controller but we feel sufficiently confident to proceed with the necessary circuit modifications to the existing amplifier on the basis of the results so far obtained in parallel with the chatter study.
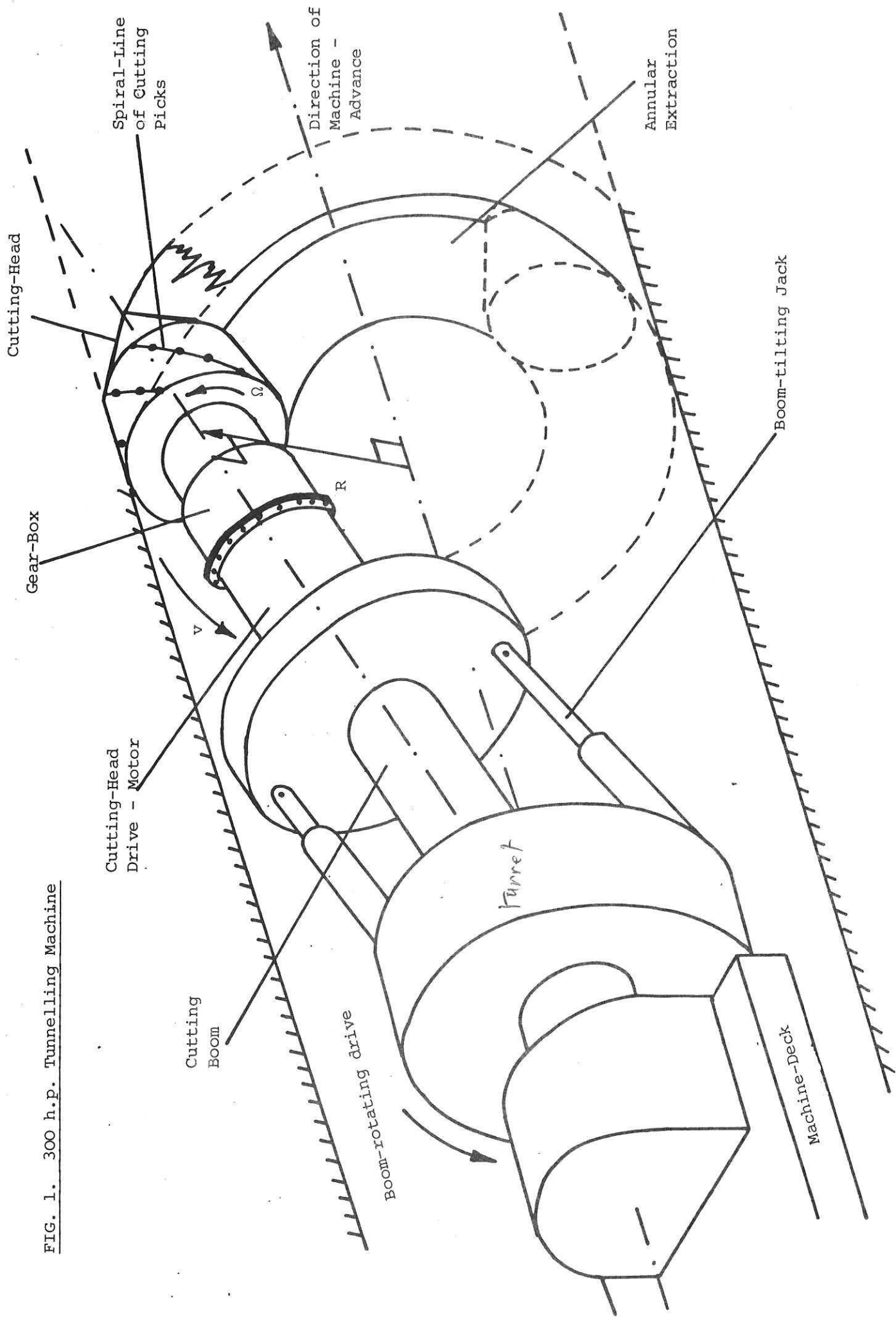
An analogue machine and servo model is under development into which the modified amplifier will be connected to test its behaviour before installation on the machine for 'before' and 'after' trials. Ideally, an intermediate test of the amplifier on a valve-loaded hydraulic power pack would be desirable also to ensure no unforeseen complications associated with the electrohydraulic servo.

If an improved overriding control is ultimately preferred to the proposed continuous controller, the required conversion should be possible without undue complication.

6. <u>REFERENCES</u>

(1) Edwards J.B.: 'Modelling the dynamics of coal and mineral cutting' Proc. I.Mech.E., 1978, Vol. 192, No. 30, pp. 359-370.

(2) Nicholson H.:(Ed. 'Modelling of Dynamical Systems, Vol II', Peter Peregrinus, I.E.E. Control Engineering Series 13, 1981, pp. 178-233.

(3) Edwards, J.B. and Owens, D.H.: 'Analysis and Control of Multipass Processes', J. Wiley (Research Studies Press), Letchworth, 1982, 298 pp.
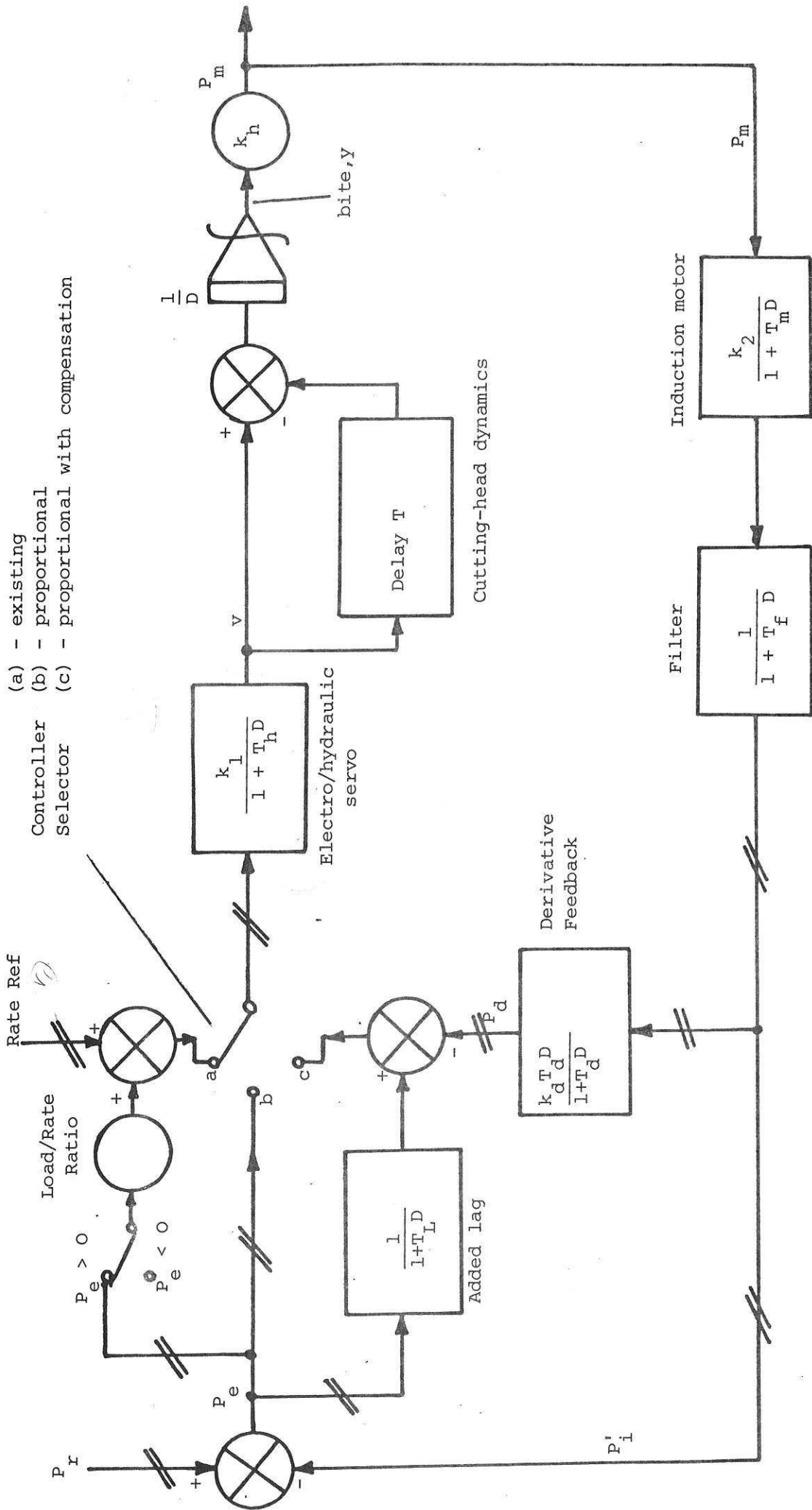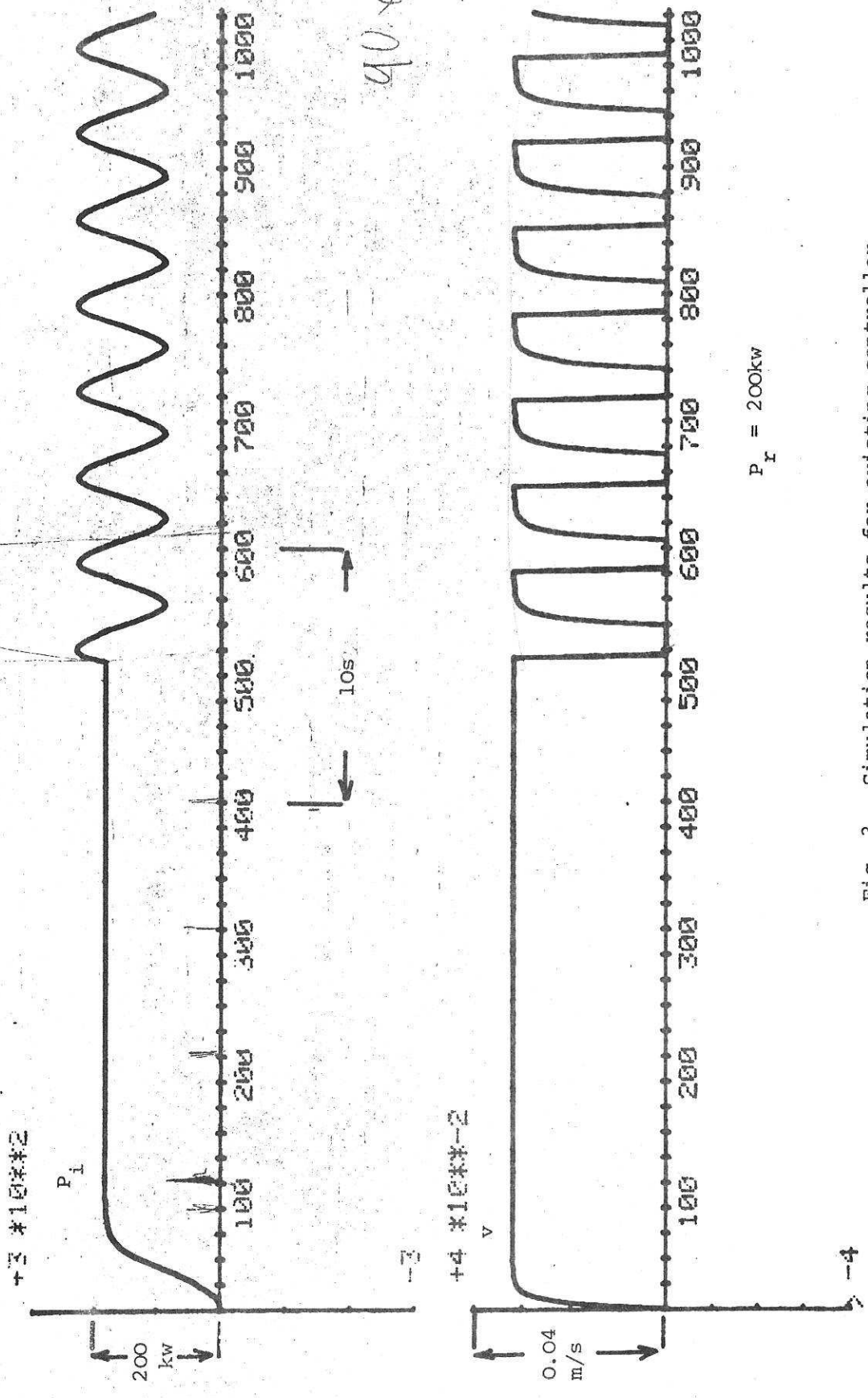
FIG. 1. 300 h.p. Tunnelling Machine

Cutting-Head

Spiral-Line
of Cutting
Picks

Direction of
Machine –
Advance

Annular
Extraction

Gear-Box

Cutting-Head
Drive – Motor

Ω

R

v

Boom-tilting Jack

Cutting
Boom

Turret

Boom-rotating drive

Machine-Deck

Fig. 2 Block Diagram of Rock-Cutting System and Alternative Controllers

R2 = 0.032
K₂ = 1
5sec

+3 *10**2
P_i
200 kw
−3

+4 *10**-2
v
0.04 m/s
−4

P_r = 200kw

Fig. 3. Simulation results for existing controller

Fig 3

Re

$\omega = 0$

Im

O

$\omega = \pi/T$

zero-ω
M-circle

Added vector $\{1 \underline{/\ 135^\circ}\}$
needed for compensation

135°

ω_c

-1

Critical point

Locus for $T_h = T_m = T_f = 0$

Note locus $\rightarrow \infty$ as $\omega \rightarrow 2\pi/T$

Compensated
System Locus

Locus of $G^{-1}(j\omega)$
for $k_1 = 0.3 \ 10^{-3} \text{m/s/kw}$
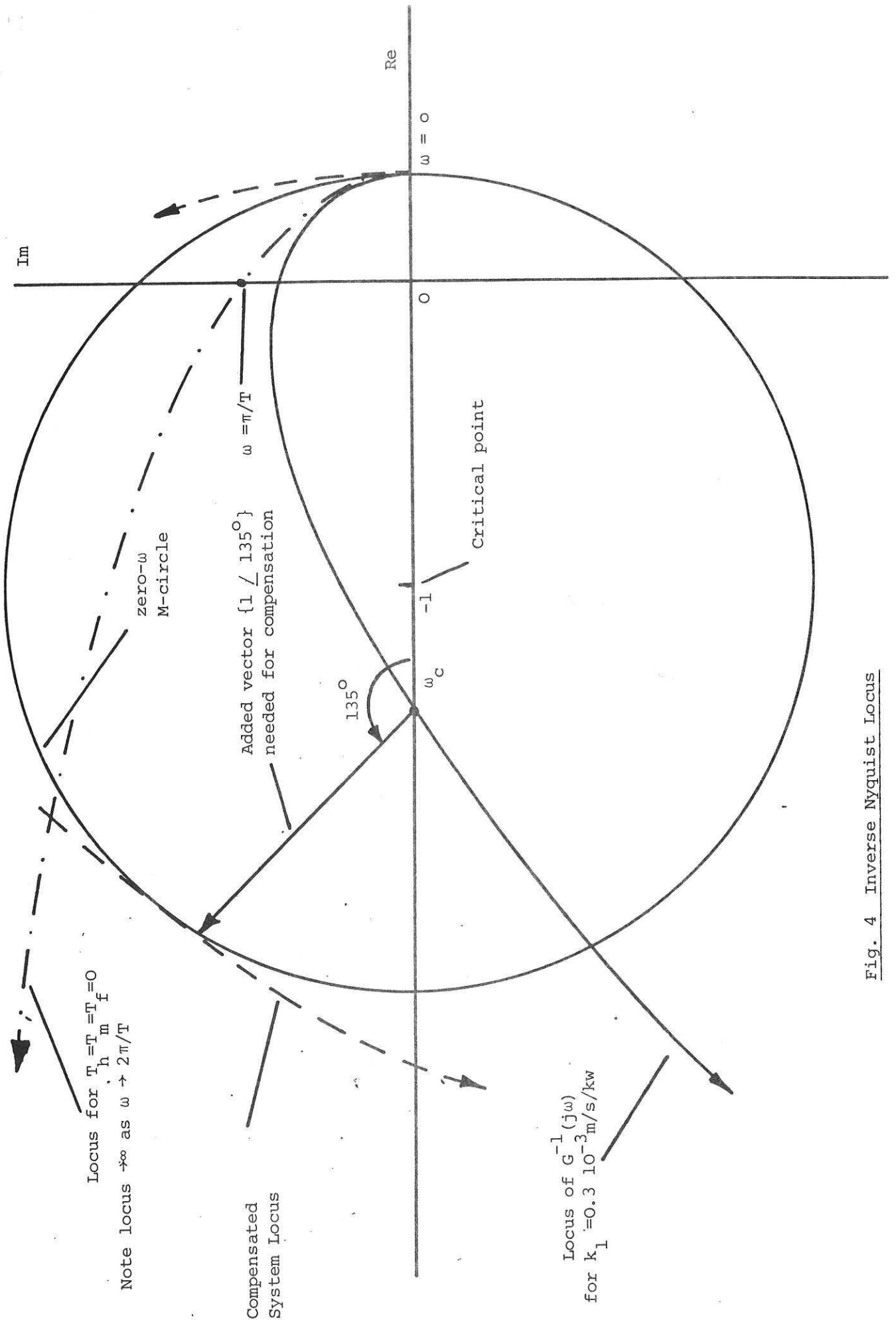
Fig. 4 Inverse Nyquist Locus

P_i

10s

200 kw

0.04 m/s

v
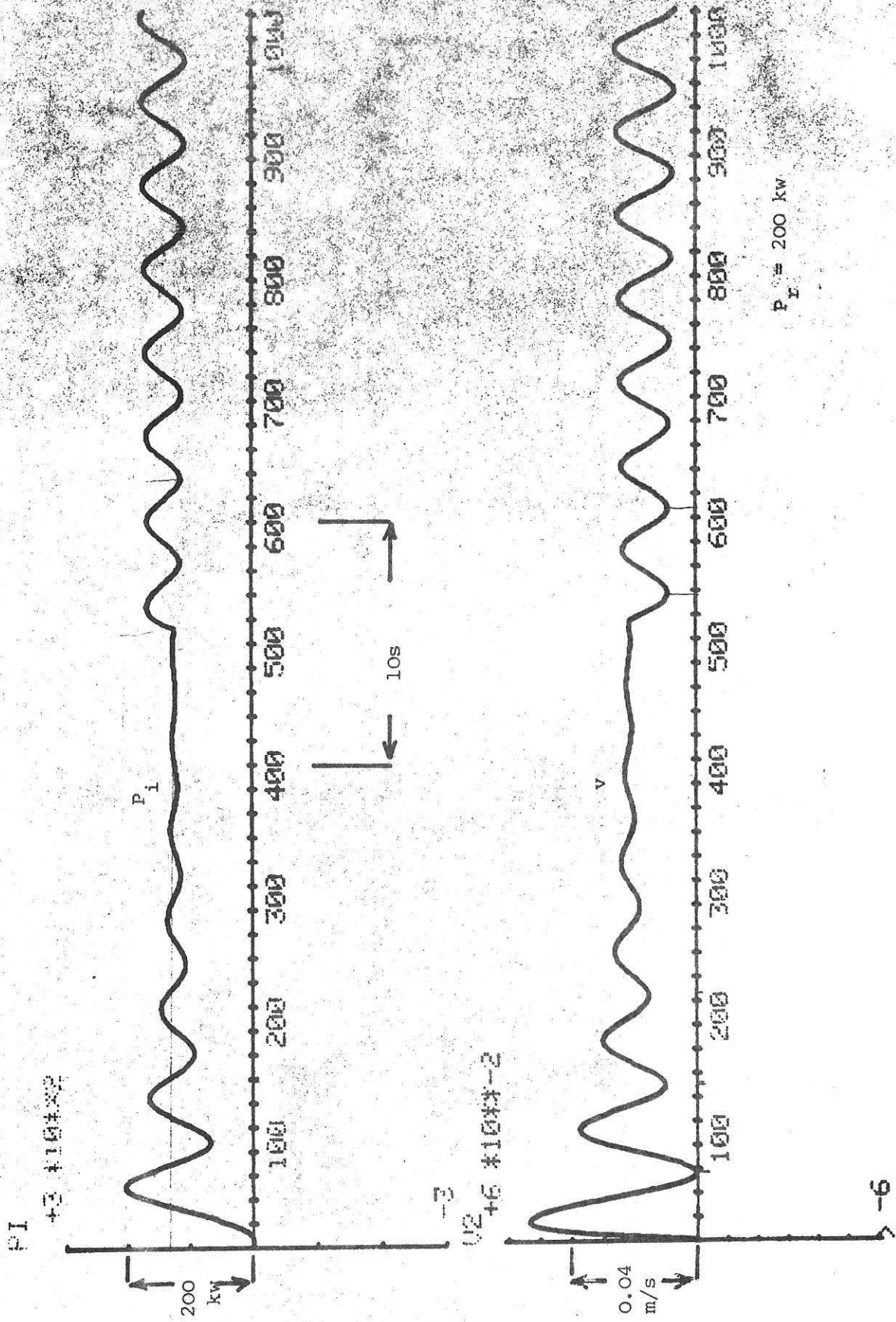
Fig. 5 Continuous controller, $k_1 = 0.3 \cdot 10^{-3}$ m/s/kw without compensation

fig 5

Fig. 6.   Proportional Controller, $k_1 = 0.15.$ 10^{-3} m/s/kw, No compensation.
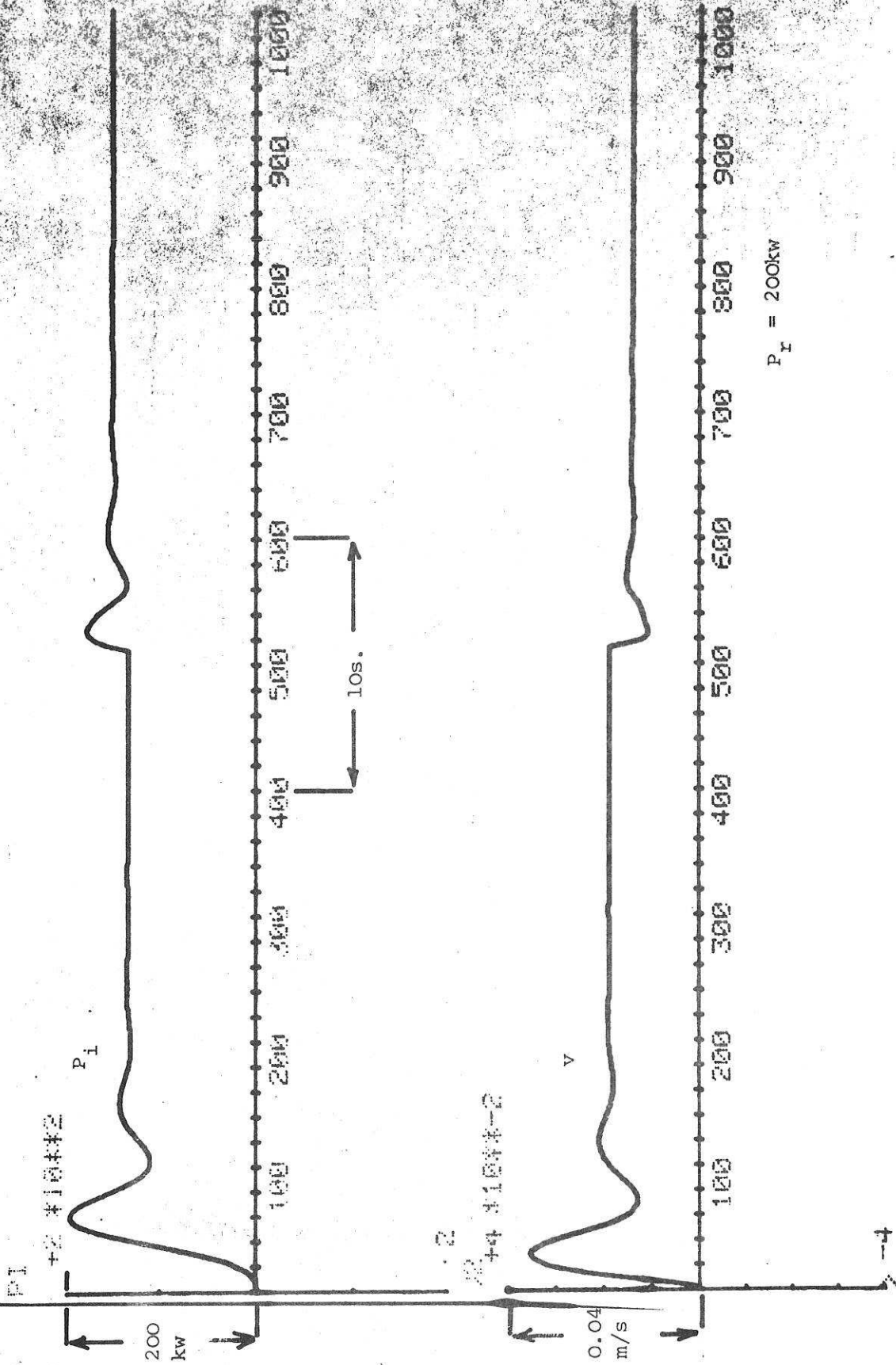
Fig. 7 Continuous controller with compensator
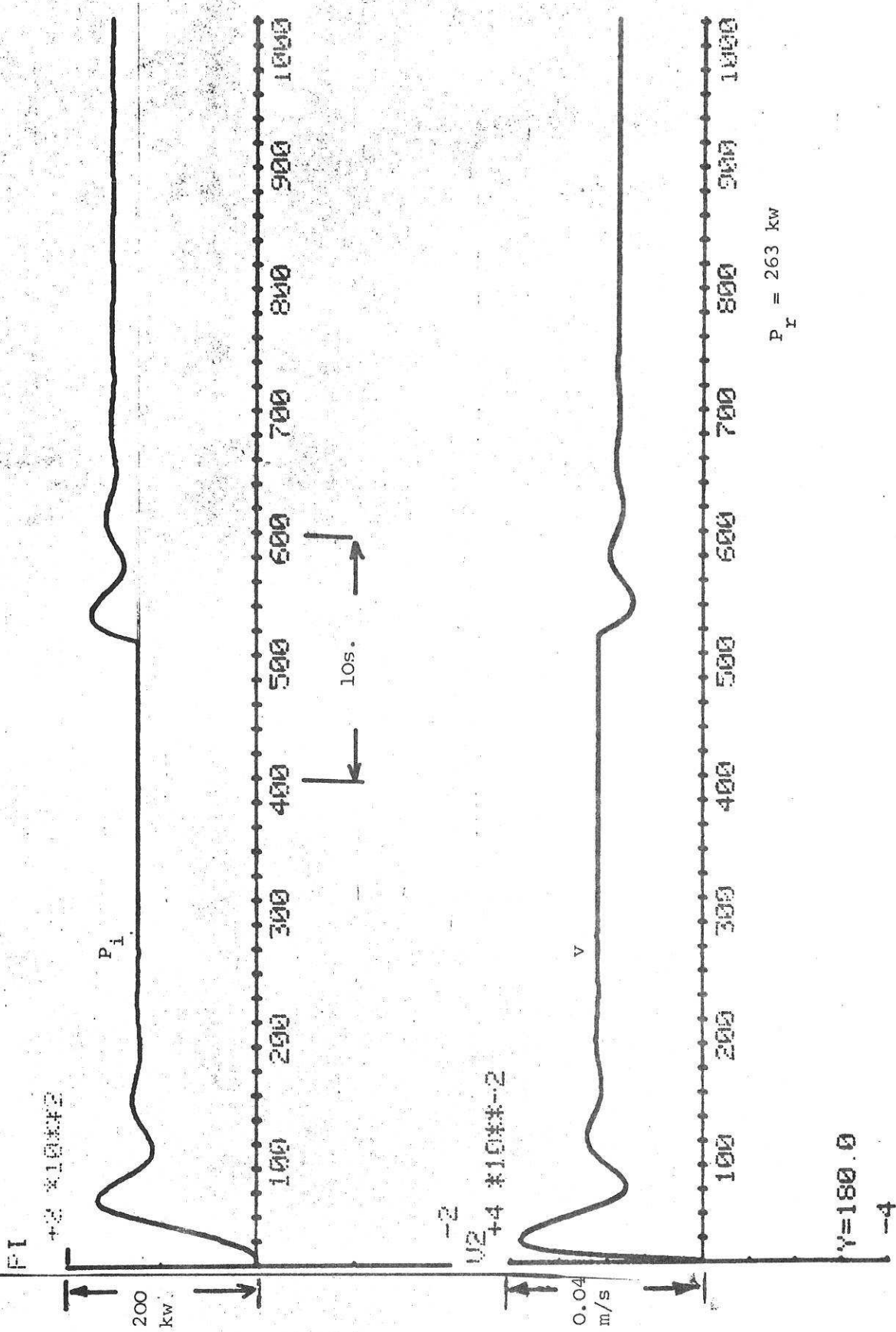
$P_r = 200kw$

Fig. 8 Continuous controller, $k_l = 0.3.10^{-3}$ m/s/kw, No compensation, increased ref.

$P_r = 263$ kw
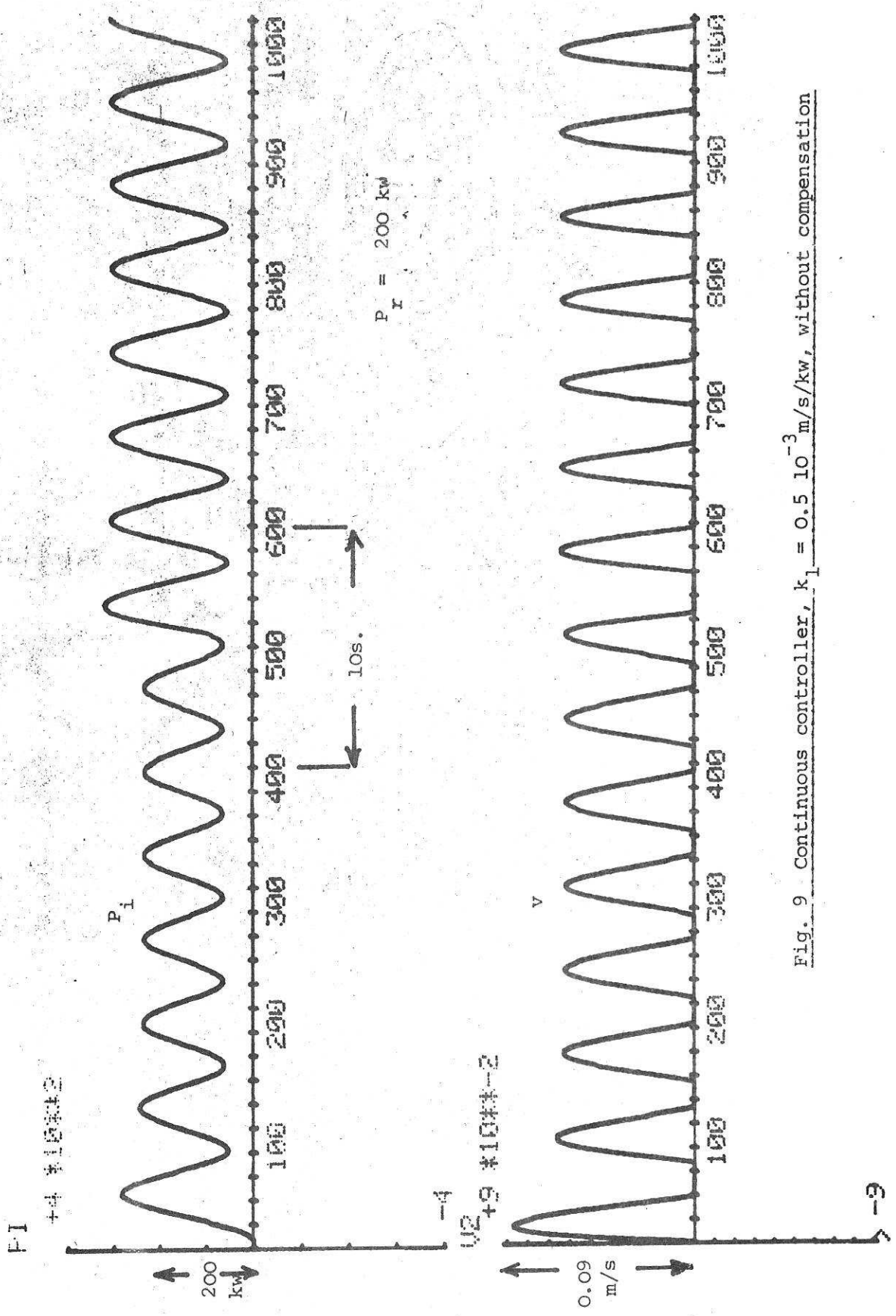
Fig. 9 — Continuous controller, $k_1 = 0.5 \cdot 10^{-3}$ m/s/kw, without compensation

$P_r = 200$ kw